Available online at www.sciencedirect.com
ScienceDirect
Chemical Physics 341 (2007) 189–199
Chemical Physics
www.elsevier.com/locate/chemphys

Anomalous phase behavior and apparent anharmonicity of the pump–probe signal in a two-dimensional harmonic potential system

T. Taneichi [a,b,*], T. Kobayashi [a,b,c,d]

[a] ICORP, JST, Kawaguchi Center Building, 4-1-8, Honcho, Kawaguchi-shi, Saitama 332-0012, Japan
[b] Department of Applied Physics and Chemistry, Institute of Laser Research, The University of Electro-Communications, 1-5-1, Chofugaoka, Chofu, Tokyo 182-8585, Japan
[c] Department of Electrophysics, Advanced Ultrafast Laser Center, National Chiao Tung University, 1001, Ta Hsueh Road, Hsinch 3005, Taiwan
[d] Institute of Laser Engineering, Osaka University, 2-6, Yamada-oka, Suita, Osaka 565-0871, Japan

Received 1 March 2007; accepted 13 July 2007
Available online 10 August 2007

Abstract

Discussion on wavelength dependent "anharmonic" effects in a pump–probe signal for a system of wavepacket on one- and two-dimensional harmonic potentials was given. The Fourier power spectrum of the signal, calculated for a model composed of a three-state electronic system coupled to a set of displaced harmonic oscillators, depends on the pulse duration. Condition under which the wavepacket motion in the harmonic potential substantially deviates from that of the classical point mass is derived. The Fourier power spectrum has enhanced components with frequencies of harmonics even in a system composed of ideally harmonic potentials. Utility of the Fourier analysis of the spectrum for clarification of the squeezed molecular vibrational state is discussed. Calculated oscillatory behavior in phase of a pump–probe signal, as a function of probe frequency, was discussed in terms of a two-dimensional effect on a pump–probe signal.

Keywords: Wavepacket; Molecular vibration; Phonon; Pump–probe spectroscopy; Phase; Fourier power spectrum; Transient spectrum; Molecular dynamics; Vibrational modes; Ultra-fast phenomena

1. Introduction

Pump–probe spectroscopy using a femtosecond laser is a powerful tool for detecting ultra-fast phenomena such as molecular vibrations [1–11], ultra-fast chemical reactions [1–3,12,13], and exciton dynamics [14–16]. The observed results often have been interpreted in terms of a wavepacket picture, by which one can set theoretical bases on the experimental results and predict novel phenomena [17–22]. A classical vibrational motion is obtained as far as the wavepacket is well localized in a vibrational coordinate and vibrational coherence is maintained. An oscillatory structure reflecting the wavepacket motion is obtained in a time-resolved pump–probe signal. A vibrational mode analysis (VMA) is based on the decomposition of the signal into several vibrational modes by the Fourier analysis [23] or the singular-value decomposition [24]. In practice, the signal may not be merely a damped sinusoidal oscillation, but it may follow a complicated dynamics such as a power law due to the process of diffusion [14,15,25–29] and a stretched exponential decay due to distributed decay rates [30]. Even for a system in which such complicated electronic state dynamics are not dominant, they have usually several modes coupled to the electronic excitation. The Fourier power spectrum is formulated and the real-time trace can be analyzed by using the harmonic oscillator model [31]. When a wavepacket is excited in a region near the equilibrium position of a certain excited state, one can approximate the bound-state potential curves under consideration as being harmonic with specified frequencies.

* Corresponding author. Address: ICORP, JST, Kawaguchi Center Building, 4-1-8, Honcho, Kawaguchi-shi, Saitama 332-0012, Japan.
E-mail address: taneichi@ils.uec.ac.jp (T. Taneichi).

0301-0104/$ - see front matter © 2007 Elsevier B.V. All rights reserved.
doi:10.1016/j.chemphys.2007.07.047

A common theoretical analysis is to use a harmonic potential as an approximation of a real bound-state potential or those closer to real such as the Morse type [32]. Under the conditions that justify this approximation, however, one needs to consider another issue concerning the excitation process: squeezing of the molecular vibrational wavepacket [33]. It is shown that a substantial difference can be obtained in the Fourier decomposition of experimental spectra for the coherent phonon and the squeezed phonon even for a system containing a realistic amount of electron–phonon coupling [34]. Assume that every mode, which is decomposed either by Fourier decomposition or by SVD, can be well-approximated by a harmonic oscillator. It is discussed that the influences from higher-order components on the VMA are inevitable, that is, there is not always one-to-one correspondence between signals obtained in VMA and vibrational modes of the system under consideration. Focusing on a single vibrational mode, the influence of higher-order components on VMA is quantitatively studied. Intensities of decomposed frequency components vary with change in the probe frequency. It is shown that one can tell, for instance, which peak obtained in VMA is the fundamental frequency component and which ones are the contributions from higher-order components, since decomposed frequency components have different dependences on probe frequency with each other.

In case two vibrational modes are taken into account, wavepacket is considered to move around on a 2D potential surface. Chemical reaction control based on the quantum optimal control simulation using model potential energy surfaces [35–37], and dependence of vibrational distribution on an electronic excited state on the intensity of excitation pulse [38] have been discussed so far. Few reports, however, have aimed at a detailed discussion on the pump–probe signal in such a system. Phase of molecular vibration has been addressed both theoretically and experimentally [31,39]. Pulse width dependent behavior of the phase as a function of probe frequency was observed that shows excellent agreement with theoretical prediction [39]. If the vibrational mode under consideration can be approximated by the harmonic potential, the phase of molecular vibration changes π at the equilibrium position. Strong deviation from this typical behavior in phase was observed in our group [40], in which the phase showed a clear oscillation as a function of the probe frequency. Part of this work is motivated by an idea that the anomalous behavior in phase is due to the wavepacket propagation on 2D potential surfaces, that is, the system is composed of a superposition of two vibrational modes. Calculation of the pump–probe signal for the 2D system is made and, based on the results, phase of molecular vibration is discussed in connection with the observation.

Squeezed molecular vibration was initially discussed as a realization of squeezing of general quantum oscillator in the molecular system. Its generation mechanisms, such as excitation with a chirped optical pulse [41], sudden change in vibrational frequencies during the Franck–Condon transition [42], and superposition of the coherent states in a one dimensional configuration [43], have been proposed. Several proposals were made for the detection of squeezed molecular state [33,41]. In this study, another proposal is made for the detection, based on the Fourier decomposition of the pump–probe signal. It is investigated whether the ratio between the intensity of the fundamental component and that of the higher-order harmonics is valid as a means for the judgment of squeezing.

Effect of the "apparent anharmonicity" that emerges in the transient pump–probe signal is discussed, in connection with vibrational scheme of molecule, in Section 2. Squeezing effect in the signal is discussed in detail based on the Fourier analysis. In Section 3, discussion of this anomalous "apparent anharmonicity" is extended to the case of two-mode system described by 2D potential surfaces. In an experiment in our group, it was observed that the phase of a pump–probe signal that oscillates with delay-time oscillates with respect to the probe frequency [40]. Two-dimensional effect on a pump–probe signal is discussed concerning this effect, in Section 4.

2. A single mode case

In this chapter, effect of phonon squeezing on the transient spectrum of a system with much smaller coupling strength, which is frequently encountered in real molecular systems is studied. In such a system, the spectra are modified due to squeezed phonons, which are visually less obvious than those discussed in Ref. [33]. We will demonstrate in this paper how the squeezing of phonons substantially influences the Fourier components of the spectrum in such realistic cases. Hereafter the intramolecular vibration is called "phonon" for simplicity.

2.1. Phonon statistics

The pump–probe signal obtained in the short-pulse limit has a Gaussian-like dependence on the probe frequency, which does not change its height during the period of molecular vibration, and vibration of the signal along the delay time is sinusoidal at any probe frequency. For a longer pulse, however, the signal changes its shape during the vibrational period, and its vibration is not sinusoidal. With a finite pulse width, therefore, contributions of the second and higher-order components of Fourier decomposition are expected to be more significant than those with the short-pulse limit. In this context, the deviation of the wavepacket formation scheme from the coherent excitation is called "apparent anharmonicity". This is due to the deviation of the quantum harmonic system from the classical one.

It was shown that the transient pump–probe spectra obtained for a molecular system is sensitive to the scheme of phonon excitation [33]. The phonon generated through optical excitation, with reciprocal pulse duration, u, in an

electronic excited state has its own quantum mechanical statistics. The statistics changes according to the amount of u relative to the vibrational mode frequency, ω, which is measured by an impulse factor, $I = u/\omega$ [39]. In the short-pulse limit, $u \gg \omega$, the system undergoes a coherent excitation, and the generated phonon exhibits a vibration well-approximated by a classical motion. In this excitation condition, the phonon is characterized by the variances of the phonon quadratures, given in terms of the phonon operators as $\widehat{X}_+ = \hat{b} + \hat{b}^\dagger$ and $\widehat{X}_- = -i(\hat{b} - \hat{b}^\dagger)$, of a coherent state as

$$\Delta X_\pm^2 = 1. \tag{1}$$

Note that $\Delta X_\pm^2$ depends only on the excitation condition, such as the pulse width and its chirp. It was shown that the phonon is maximally squeezed at $u \approx 4\omega$ as far as Gaussian pulses are used [33], where the variances are determined as

$$\Delta X_+^2 \approx 0.31, \tag{2}$$

and

$$\Delta X_-^2 \approx 4.0. \tag{3}$$

Here $\Delta X_\pm^2$ are evaluated just after the Franck–Condon transition, at which ΔX_+^2 is known to take its minimum value when the molecular vibration is squeezed. While a remarkable change in the profile of the spectrum due to the distribution of phonon was clearly shown [33], the electron–phonon coupling used in this calculation exceeded that observed in actual molecular systems.

2.2. Fourier analysis of the transient spectrum

The molecule is initially assumed to be in its electronic ground state $|1\rangle$. Molecular system is assumed to be composed of three electronic states coupled to a set of displaced harmonic oscillators. The pump and probe pulses interact with different electronic transitions; that is, the pump generates a population at the first excited state $|2\rangle$, while the probe is responsible for the transition between $|2\rangle$ and the second excited state $|3\rangle$. The transient spectrum is defined as the population in $|3\rangle$, p_3, formulation for which is given in appendix.. The transient spectra, defined by p_3 as a function of the delay time and probe frequency, are calculated for pulse widths between the cases of the nearly coherent phonon ($u = 8\omega$) and the quasi-number state phonon ($u = \omega$), including the one close to most efficiently squeezed phonon ($u = 4\omega$). The calculations are performed for the weak ($g_{12} = g_{23} = 1$) and the strong ($g_{12} = g_{23} = 3$) electron–phonon coupling regimes. Phonon squeezing is shown to change the transient spectrum substantially, reflecting the deviation of the molecular vibration from a classical analog of vibration.

The spectrum for a squeezed phonon exhibits an oscillatory change in its width and shape due to the periodic reduction/expansion and expansion/reduction of the wavepacket associated with the molecular vibration coordinates and conjugate momenta, respectively. The transient spectrum changes its peak position during the vibrational period, according to the wavepacket motion on the first excited potential curve. It was shown in Ref. [33] that the transient spectrum changed its width during the period of vibration. In contrast, such a squeezing effect in the width is not clear in our case, where the electron–phonon coupling is much smaller. This is a distinct feature of the weak coupling regime, which was not discussed in Ref. [33]. To elucidate the effect of phonon squeezing on the spectrum, Fourier transformation against the delay time is applied to p_3 for each probe frequency given as a function of the delay time, from which relative contributions of harmonics are estimated. The results on the pulse duration of $u = 4\omega$ for the strong coupling regime ($g_{12} = g_{23} = 3$) are shown in Fig. 1. The probe central frequency, ranging from -13ω to 20ω, is expressed as a difference from the electronic gap between the minima of two relevant potential curves. One can see a dominant component of the fundamental frequency, ω. Another component corresponding to 2ω, also detectable, has a peak corresponding to the double-frequency region that lies around the equilibrium position of the potential. This is because the wavepacket passes through this region twice in each period of vibration. The wavepacket, on the other hand, passes the turning points once in each period, leading to the two main peaks in the fundamental order component at the probe frequencies resonant to the turning points.

These are common features observed in any case of the pulse duration and coupling strength in the present formulation. The spectrum changes its shape during the vibrational period as far as the excitation pulse has a finite width, and consequently the excited vibration is neither in a vibrational coherent state nor a vibrational eigenstate. As a general feature, generation of high harmonics is enhanced in a stronger coupling regime. This is because the change in the spectral shape is more significant in the case of stronger electron–phonon coupling. This change in the shape includes an oscillatory change in the width

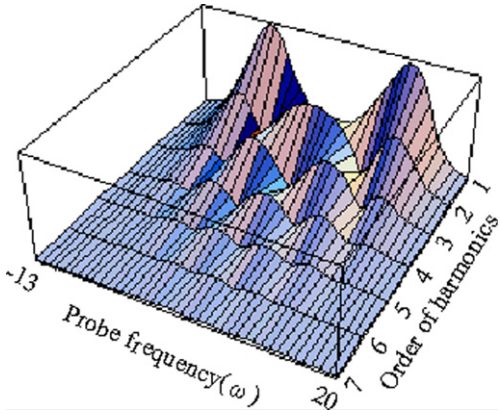

Fig. 1. Plots of Fourier transformation applied to the delay time-dependent spectrum for the strong coupling regime in the case of $u = 4\omega$.

of an asymmetric profile, which leads to a deviation of the temporal vibration of each point of the spectrum from a sinusoidal one.

The contribution of the second and higher-order harmonics components to the spectrum, integrated over the probe frequency, is evaluated by the ratio to that of the first order, as plotted in Fig. 2. A comparison is made for the pulse width ranging from 0.5ω, which corresponds to the long-pulse limit generating nearly vibrational eigenstate, to 8ω, the short-pulse limit leading to a coherent excitation. A comparison with the strong electron–phonon coupling regime is also made. In both cases, the high harmonics components are remarkably enhanced with an intermediate pulse width characterized by the most efficient squeezing condition ($u = 4\omega$). It is also seen that, especially in the strong coupling regime, the contribution of higher harmonics is not negligible when the pulses are short enough to excite a coherent phonon.

2.3. Phonon characterization

The contribution of higher harmonics is plotted as a function of the pulse width in Fig. 3. Here R is defined as $R = I_s/I_f$, where I_f and I_s are the integrated Fourier power spectrum in terms of probe frequency of the fundamental and the second harmonic, respectively. Each contribution is estimated by integration along the probe frequency estimated in Fig. 2. Note that only the second harmonic component is selected in this estimation for a practical reason: it is difficult to evaluate the effects of third and higher-order contributions quantitatively from a noisy pump–probe signal.

Oscillation of a signal along the delay time at each probe frequency, excited with a pulse of finite width, makes a more contribution of the second and higher-order components of Fourier decomposition than that excited with a short-limit pulse. On the other hand, no wavepacket is generated in the long-pulse limit; only a single vibrational level is excited under this condition. In this limit the obtained signal has no delay-time dependence. In this respect, one can understand that R, as a function of the pulse width, has a maximum at a certain point, as displayed in Fig. 3. Squeezing also has its maximum at $u \approx 4\omega$ [33].

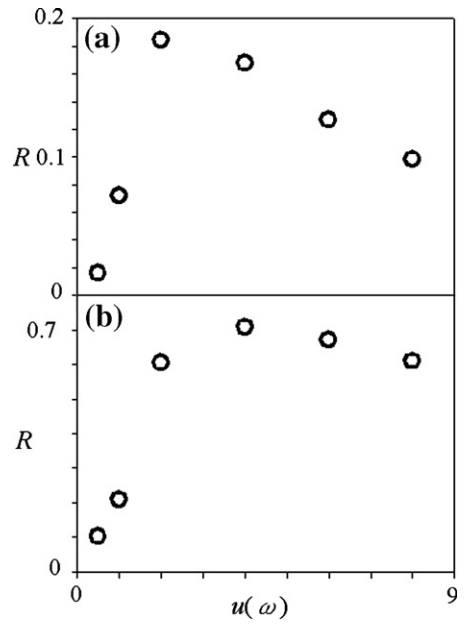

Fig. 3. Dependence of R on the pulse width: (a) $g_{12} = g_{23} = 1$ and (b) $g_{12} = g_{23} = 3$.

For experimental identification of the squeezed phonon, squared variance of phonon quadratures, ΔX_+^2, is plotted in Fig. 4 as a function of R for both weak and strong coupling regimes. In both cases, ΔX_+^2 is less than unity for larger R; that is, the molecular wavepacket is squeezed. In other words, one can confirm the squeezing by determining the relative contributions of higher harmonics to the observed pump–probe transient spectrum in such a system

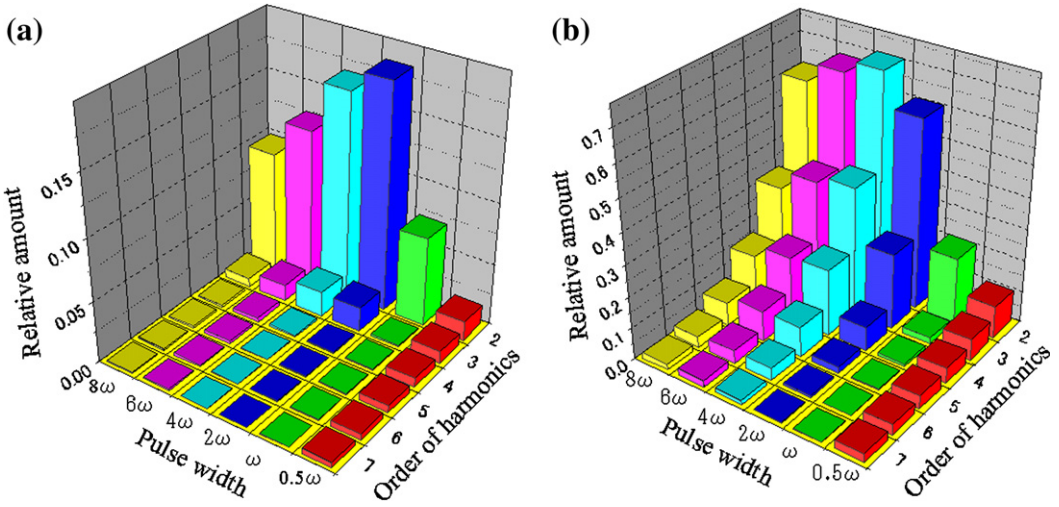

Fig. 2. Ratios of each harmonics component to the fundamental ω component: (a) $g_{12} = g_{23} = 1$ and (b) $g_{12} = g_{23} = 3$.

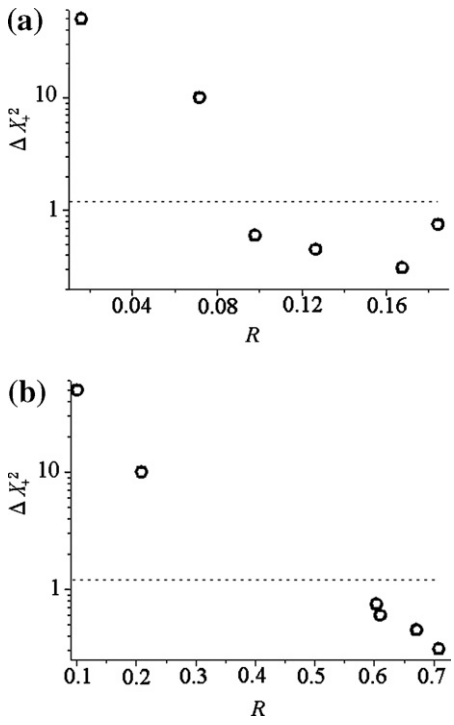

Fig. 4. Squared variance of phonon quadratures as a function of R. (a) $g_{12} = g_{23} = 1$ and (b) $g_{12} = g_{23} = 3$.

that is precisely described by harmonic potentials. It is shown that a Fourier power analysis can be used for detecting the squeezing of molecular wavepacket in the range of electron–phonon coupling strength covered in this work.

To summarize, statistical features of a wavepacket of molecular vibration affect the pump–probe transient spectrum. We have demonstrated a substantial difference in the Fourier decomposition of experimental spectra for the coherent phonon and the squeezed phonon even for a system containing a realistic amount of electron–phonon coupling. Therefore, one needs to be careful in a frequency analysis of molecular vibration, which can be modified by a deformed molecular vibrational wavepacket.

As discussed above, the possibility that a single vibrational mode behaves like two modes in a mode analysis increases when the condition of excitation satisfies that of creating a squeezed phonon. We have shown that Fourier analysis of an observed spectrum can manifest generation of a squeezed molecular vibrational state. As a counterpart of the present theoretical study, where only a single vibrational mode is considered, spectroscopic studies have been made, in many cases, on more complicated samples such as polymers and metal complexes containing many vibrational modes. In such a practical measurement, decomposition to single modes and estimation of their Fourier components are much harder because of the modes lying close to one another and coupling effects among them. A pump–probe experiment on a simpler system such as a diatomic molecule using a sub-5fs laser system seems to be the first feasible approach to overcome this problem.

3. A two-mode system

Let us consider a two-mode system. Photo-induced dynamics of the wavepacket on 2D potential energy surfaces is obtained in the time-dependent picture based on the Schroedinger equation numerically solved on a grid using the second-order operator splitting method [44]. The fast Fourier transform method is employed to evaluate the propagator of the nuclear kinetic energy operator. Our system is composed of three electronic states, $|g\rangle$, $|e\rangle$, and $|f\rangle$, on which the wavepacket propagates. Initially, the system is in the vibrational ground states of $|g\rangle$ in both modes I and II. The system undergoes $|g\rangle \rightarrow |e\rangle$ and $|e\rangle \rightarrow |f\rangle$ optical transitions in pump and probe processes, respectively. Delay-time dependence of the absorption probability of probe pulse is obtained for probe frequencies that range from $-2\omega_1$ to $2.5\omega_1$, where ω_1 is the frequency of mode I, that cover the dynamic range of the signal. Pump pulse is assumed be resonant to the $|g\rangle \rightarrow |e\rangle$ transition. In the following, probe frequency $\Delta\omega_r$ is expressed as a deviation from the energy difference between vibrational ground states in $|g\rangle$ and $|e\rangle$. Huang-Rhys factor is fixed to 0.5 at each mode and transition.

3.1. Analysis based on the Fourier power spectra

We have shown in the previous chapter that the vibration of signal obtained by the pump–probe spectroscopy does not always consist of the fundamental frequency of the molecular vibrational mode under consideration, but can contain higher-order components even in the ideally harmonic systems [34]. In this study, it was found that the contribution of these "higher-order" components depends on the central frequency of the probe pulse and on the vibrational scheme of the molecular vibrational wavepacket that was created by the pump pulse. Vibrational scheme is determined only by the relation between the mode frequency and the pulse width, and can be characterized by the impulse factor, I, defined by [39]

$$I = \frac{u}{\omega}, \tag{4}$$

where u is the reciprocal pulse duration defined in Eq. (A.7), and ω is the vibrational mode frequency. If the pulse width is considerably shorter than the period of vibration, the system is excited coherently, which can be described by well-localized vibrational wavepacket. If the pulse width is sufficiently longer than the vibration period, on the other hand, only a single vibrational eigenstate is excited, without forming a wavepacket. When the molecular vibration is squeezed, maximally localized states of the two quadrature components of the vibrational wavepacket emerge temporally alternatively, in the vibrational degree of freedom. It was shown that, from the ratio between contributions of the first and higher-order components, one could clarify the squeezing of the wavepacket in the case of single vibrational mode in the previous chapter. First, the Fourier

power spectra of pump–probe signal obtained for the case in which molecular vibration of one of the two vibrational modes (mode II) is squeezed.

Prior to discussion of squeezing, Fourier power spectra of the signal expected to the pump probe experiment in which the probe frequencies are resonant to the turning and equilibrium positions of the vibration are shown in Fig. 5, for the cases of $\omega_2 = 1.5\omega_1$ and $\sqrt{2}\omega_1$. It is obvious that, similar to the single mode, one cannot neglect the contributions from components other than fundamental one, and that the amounts of higher-order contributions depend on the probe frequency. It is also similar to the case of single mode that the contributions from the third and higher-orders are negligibly small. Note that, depending on the probe frequency, either second harmonic or difference- as well as sum-frequency components are obtained. It has been shown in our previous analysis [34] that larger contributions from the second and higher-order were obtained for probe frequency in resonance to equilibrium position of vibration. In the case where two modes of vibration is taken into account, as one can see from Fig. 5, the second harmonic components of both modes have considerable contributions to the signal in the same region of probe frequency. Sum and difference frequency components, on the other hand, are the main constituents of the signal, in addition to the fundamental frequency components, for probe frequencies in resonance to the turning points of vibration, of both higher and lower sides in energy region. This is a contrasting feature of the present system to the case of single mode in which one can resolve only the sum-frequency component as the second harmonic one even in the energy region that are resonant to the turning points as well as equilibrium position. It is suggested that, based on a multi-mode pump–probe signal, one can tell which mode frequencies are contributing to the data under consideration, by comparing the Fourier power spectra obtained at the turning and the equilibrium position of the vibration, that is, the Fourier power spectrum obtained at the probe frequency resonant to the equilibrium position is composed of the fundamental and the second-order components and the one obtained at the region of turning position, on the other hand, is composed of the sum frequency component in the higher and the difference frequency one in the lower energy region in place of the second-order one, in addition to the fundamental order component. Therefore, one needs to be cautious about the possibility that a measured signal, which has a complicated profile composed of several Fourier components in its appearance at single probe frequency, may be interpreted in terms of relatively small number of modes.

Effect of squeezing of phonon, in a case of single mode, appears in the Fourier power spectrum of the pump–probe signal. The ratio R increases with the squeezing of phonon as was discussed in the previous chapter. Let us suppose that the envelope function of the pump pulse is defined as $\exp\left[-\frac{u^2(t-t_0)^2}{2}\right]$, where t_0 is time of the pulse peak. The phonon is known to be maximally squeezed when pulse width satisfies $u \simeq 4\omega$, where ω is the mode frequency [33]. In the present study, $u = 10\omega_1$, which leads to a well-localized

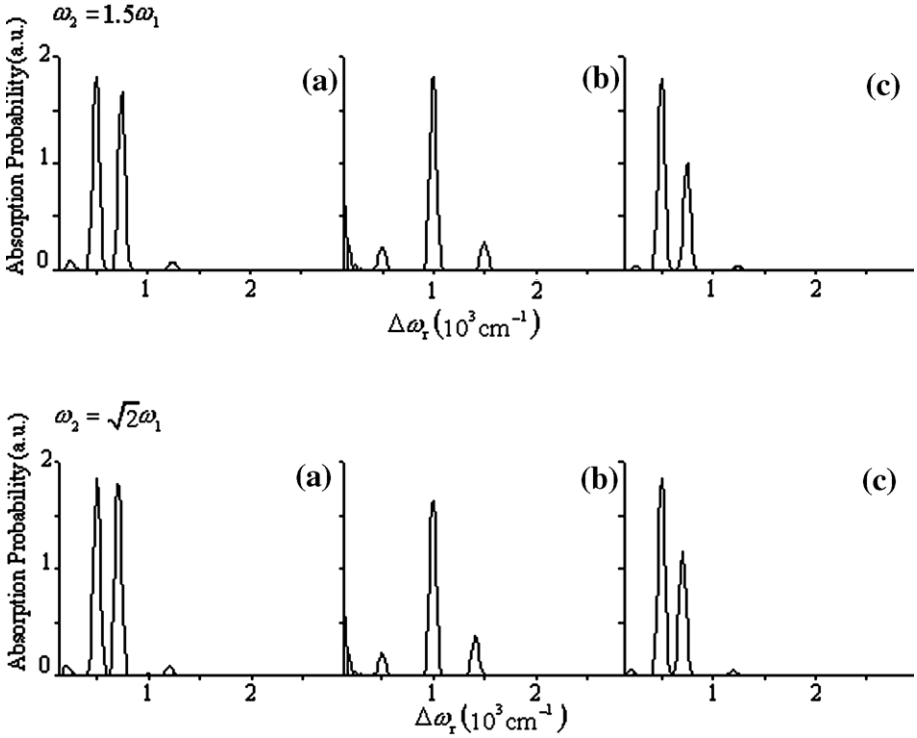

Fig. 5. Fourier power spectra of the signal in which the probe frequencies are resonant to the turning positions in the lower (a) and higher (c) energy regions, and equilibrium positions (b), of the vibration, for the cases of $\omega_2 = 1.5\omega_1$ and $\sqrt{2}\omega_1$.

coherent phonon in the mode I. In mode II, on the other hand, phonon is squeezed if $\omega_2 = 2.5\omega_1$ is satisfied. R is calculated, which is shown in Fig. 6, for $\omega_2 = 2.5\omega_1$ together with other ω_2's, for comparison. It is shown that, in contrast to the single mode system, R decreases monotonically with the ratio of mode frequencies and no signature of squeezing that appears as a considerable increase in R for the case of single mode, is seen. It is, therefore, concluded that one can no more judge correctly if the phonon is squeezed, based on R in the pump–probe signal obtained from multi-mode intramolecular system.

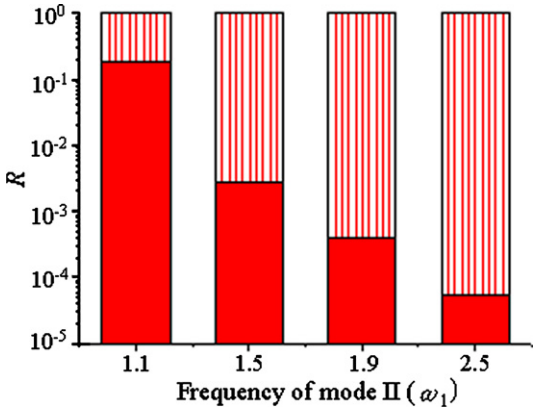

Fig. 6. R as a function of ω_2 for $\omega_2 = 1.1\omega_1$, $\omega_2 = 1.5\omega_1$, $\omega_2 = 1.9\omega_1$ and $\omega_2 = 2.5\omega_1$ (squeezed).

4. Oscillation in probe-frequency dependent phase

Let us consider the oscillatory behavior of the phase of the pump–probe signal as a function of probe photon energy. In order to determine the vibrational phase, p_θ, delay-time dependent absorption probability, which is measured by the population generated in $|f\rangle$ through the interaction with the probe pulse, is fitted with the following sinusoidal function for each probe photon energy:

$$p_A \cos(p_\omega t + p_\theta) + p_{slow}. \quad (5)$$

Here p_A, p_ω, p_θ and p_{slow} are the amplitude, frequency, phase of the oscillation and slow decaying amplitude, respectively. Detailed discussion on the phase of molecular vibration is given in Refs. [31,39]. Phase of the signal obtained in the single mode system is characterized as a π jump at the equilibrium position (Fig. 7). Observation

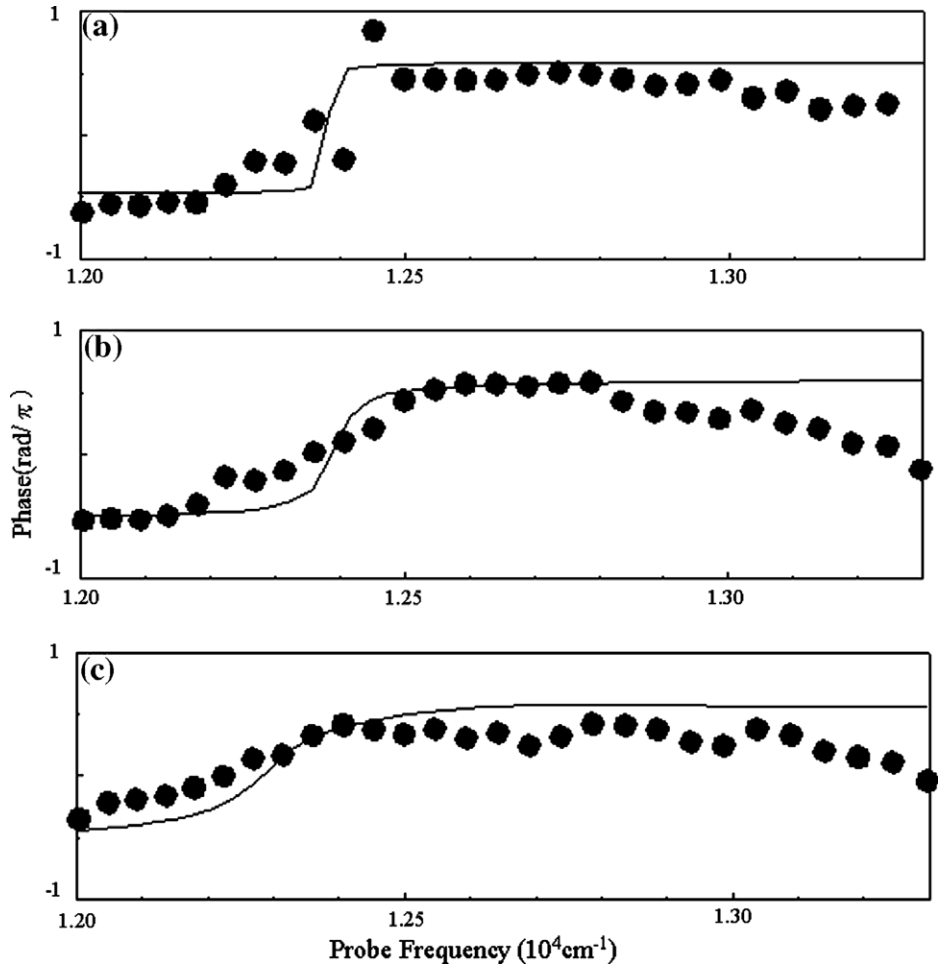

Fig. 7. Observed and calculated plots of the phase dependence on the probe frequency for three modes [39]. Solid dots and solid lines show the observed and calculated phases, respectively. Mode frequencies are: (a) 140 cm^{-1}, (b) 440 cm^{-1}, and (c) 730 cm^{-1}.

was made for a cyanine dye sample [39]. The pulse width was 20 fs. Vibrational phases obtained for three vibrational modes that have different frequencies are shown. Due to the change in relation between pulse width and the mode frequencies, probe-frequency dependent behavior in phase changes substantially, but is essentially characterized by the π shift at the equilibrium position of the molecular vibration. Let us consider a system, which consists of two vibrational modes (modes I and II) with frequencies ω_1 and ω_2 ($>\omega_1$), respectively. If the ratio of these frequencies is an integer, mode II vibrates the integer times during one period of mode I. If the frequency ratio is rational, vibrations of modes I and II synchronize with a period identical to the least common multiple of periods of both modes. In these cases, the orbit in the 2D potential is known to be a closed curve, that is, the Lissajous' curve. Consider the simple case in which frequency ratio is an integer. Mode II oscillates integer times during one period of mode I, leading to the integer number of oscillation in phase, which corresponds to the vibration in mode II, in the region of probe frequency resonant to both of the modes. As a consequence, the phase, obtained by fitting the signal for several periods of signal, is expected to show an oscillatory behavior due to the superposition of the two modes. The phase of superposed modes is calculated as a function of the probe frequency. The results are shown in Fig. 8, for the cases in which the frequency ratios are integer, rational, and irrational for comparison. It is obvious that, in the range of frequency ratio considered in the present study, the observed oscillatory behavior in the phase as a function of the probe frequency is not obtained in every case. As a result, the phase does not behave in a considerably different way from that of single mode case.

Another origin of deviation of phase behavior from that in single mode case is considered to be due to different resonance condition in these two modes, that is, difference in the resonance energies among two modes leads to a shift in probe frequency of phase jump (typical π jump in the single

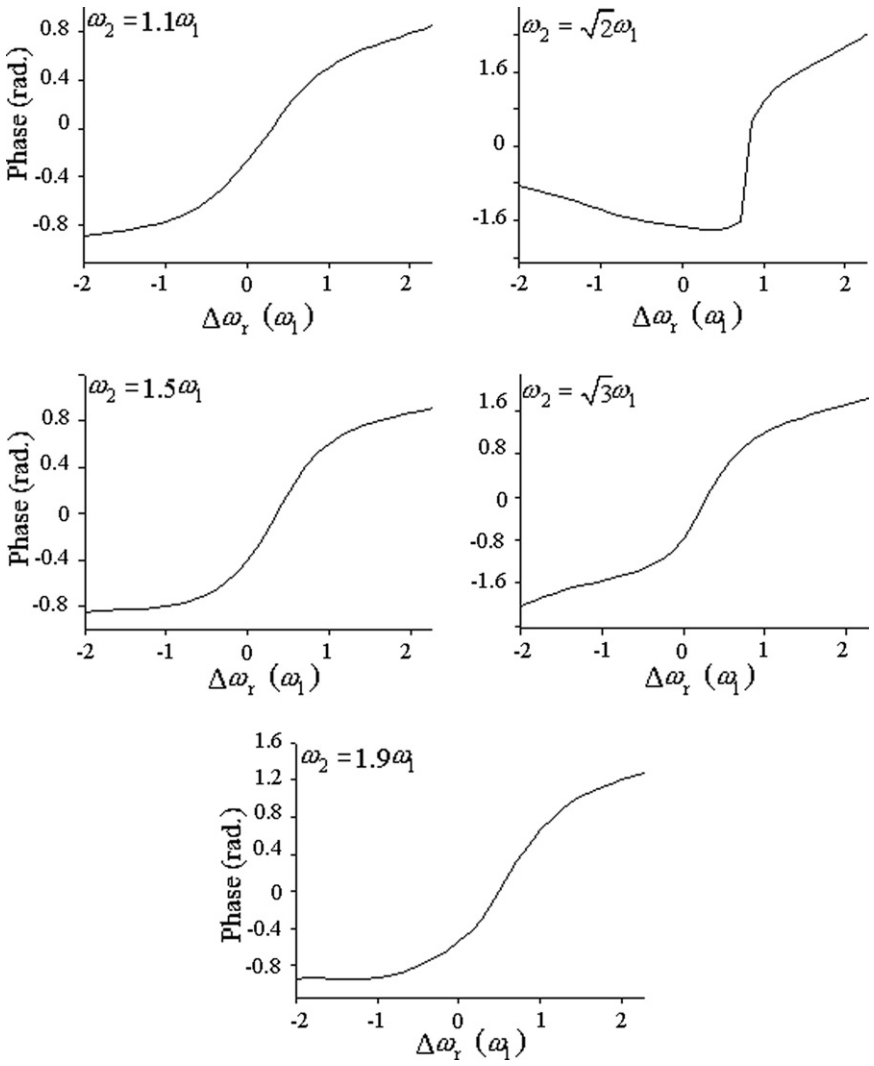

Fig. 8. Phase of superposed modes calculated as a function of the probe frequency, for the cases in which the frequency ratios are integer, rational, and irrational.

mode system is seen in Fig. 7), resulting in the change in the behavior of phase. Phase is calculated for a case in which resonance condition for the probe process ($|e\rangle \rightarrow |f\rangle$) is different among modes while keeping the resonance condition for the pump process ($|g\rangle \rightarrow |e\rangle$) identical to the previous calculation, that is, resonant to the pump pulse. Here the probe pulse is assumed to be resonant to the probe process in mode I, while it is not, on the other hand, in mode II (Fig. 9). A parameter $\Delta\Omega \equiv \Omega_{\mathrm{res}}^{\mathrm{equi}} - \Omega_{\mathrm{offres}}^{\mathrm{equi}}$, where $\Omega_{\mathrm{res}}^{\mathrm{equi}}$ and $\Omega_{\mathrm{offres}}^{\mathrm{equi}}$ are the vertical energy gaps between $|e\rangle$ and $|f\rangle$ of mode II at the equilibrium position of $|e\rangle$ of resonant and off-resonant cases, respectively, is amount of off resonance in unit of the frequency of mode I ω_1. Roughly three types of probe-frequency dependence is identified; (1) phase undergoes π shift at the phase jump points (PJP's) of both modes and 2π overall shift ($\omega_2 = \omega_1, \Delta\Omega = 1.4\omega_1$), (2) phase undergoes π overall shift with one or two PJP ('s) ($\omega_2 = 1.5\omega_1, \Delta\Omega = 1.4\omega_1$, etc.), and (3) phase derived at higher probe frequency is identical to the one at lower probe frequency with two PJP's ($\omega_2 = 2.0\omega_1, \Delta\Omega = 0.5\omega_1$). Absorption probability (AP) of the probe pulse as a function of probe frequency and delay time is shown in Fig. 10, in order to discuss the phase that is identical across two PJP's. PJP of AP corresponding to the molecular vibration in mode I is obvious when $\Delta\omega_r = 0.5\omega_1$ is satisfied, and one can also see that AP splits at $\Delta\omega_r = 0$ (indicated by a

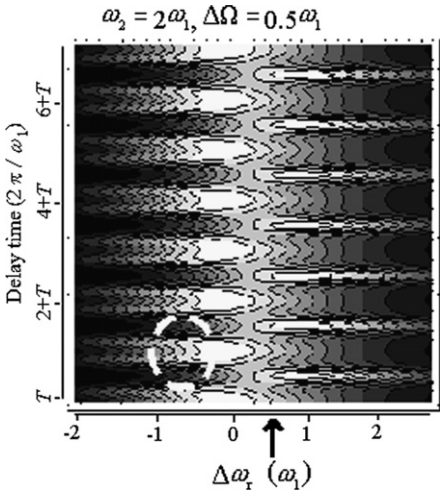

Fig. 10. Absorption probability of the probe pulse as a function of probe frequency and delay time.

circle), which corresponds to the equilibrium position of mode II with $\Delta\Omega = 0.5\omega_1$, pointed by an arrow. It is comprehensible qualitatively, from Fig. 10, for the phase to be identical in lower and higher energy region due to the split.

As a whole, the vibrational phase as a function of probe frequency is no longer monotonic in the case of 2D system, but shows a variety of probe frequency dependence

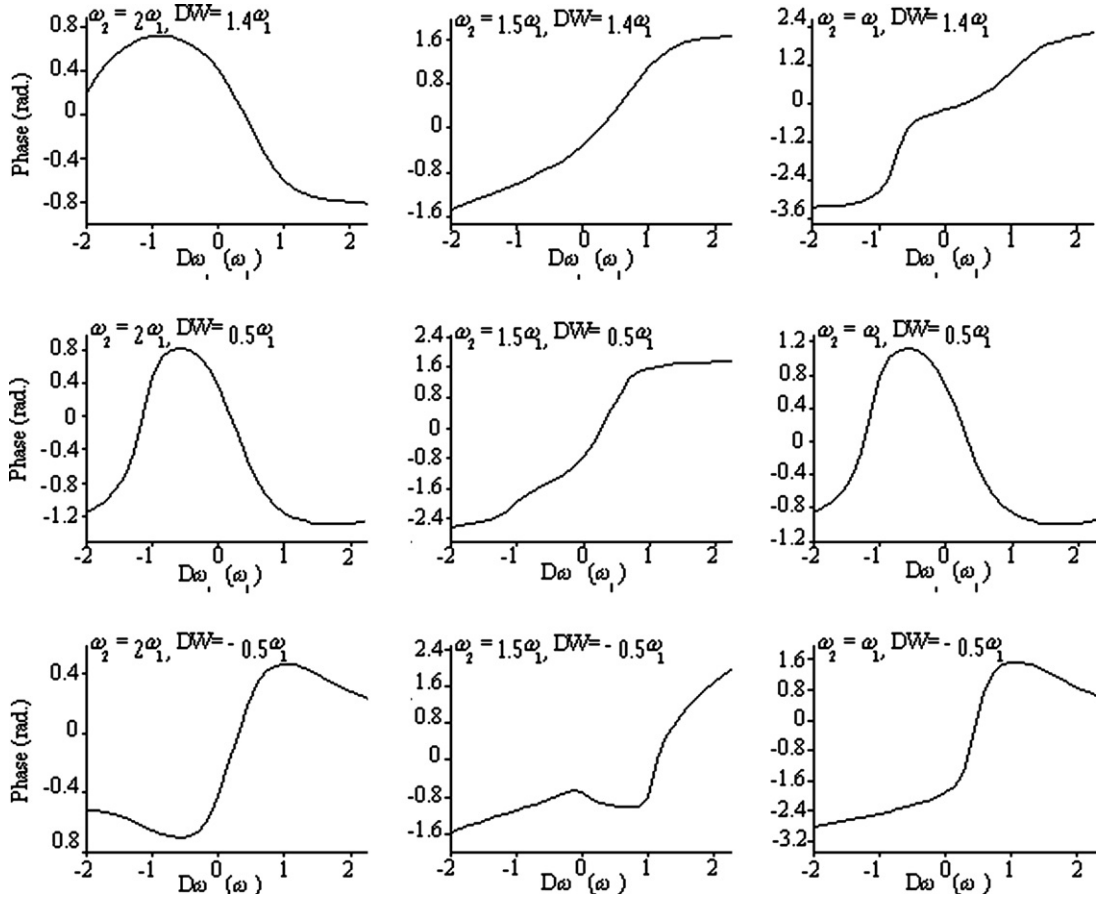

Fig. 9. Phase calculated for a case in which resonance condition for the probe process is different among modes while pump pulse is in resonance.

including successive rising and falling. Although change in the behavior of phase cannot be related to the excitation conditions, such as detuning and frequency difference among modes, in a definitive way, one can rationally conclude that the oscillation in the observed phase is due to the multi-mode effect in molecular vibration.

5. Conclusion

In conclusion, statistical feature of the molecular vibrational wavepacket is shown to affect the pump–probe spectrum. Remarkable difference is seen in the Fourier decomposition of spectra for the coherent phonon and the squeezed phonon even in case the electron–phonon coupling is of realistic amount. One has to be careful in the frequency analysis of molecular vibration which can be modified due to the deformed molecular vibrational wavepacket. Concerning the results obtained in our discussion, the possibility for which a single vibrational mode behaves as two modes during the mode analysis increases if the excitation condition satisfies that of creating squeezed phonon. It is shown that, for multi-mode system, in contrast to the single mode one, the Fourier power analysis of a pump–probe signal is no more adoptive in telling whether the system is in the squeezed state. A novel oscillatory behavior in the probe-frequency dependent vibrational phase is discussed and is shown that it is possible to interpret it as a consequence of multi-mode effect. In a system that can be approximated well by a harmonic potential in a single vibrational mode, one can clarify squeezing phenomenon by studying the contribution of high harmonics to the observed pump–probe spectrum. However, the same is not valid for the system if it has multi-dimensional potential surfaces.

Acknowledgements

This work was supported by a Grant-in-Aid for Science Research in a Priority Area "Super-Hierarchical Structures" from the Ministry of Education, Culture, Sports, Science and Technology, Japan.

Appendix A

Transient spectrum is obtained as follows. The Hamiltonian is given as

$$\widehat{H} = \widehat{H}_0 + \widehat{V}(t), \tag{A.1}$$

where

$$\widehat{H}_0 = \sum_i \varepsilon_i \hat{a}_i^\dagger \hat{a}_i + \sum_{i\lambda} \hbar\omega_\lambda c_{i\lambda} (\hat{b}_\lambda^\dagger + \hat{b}_\lambda) \hat{a}_i^\dagger \hat{a}_i + \sum_\lambda \hbar\omega_\lambda \hat{b}_\lambda^\dagger \hat{b}_\lambda \tag{A.2}$$

is a molecular Hamiltonian composed of three electronic states coupled with a phonon. Here $\hat{a}_i$ and $\hat{b}_\lambda$ denote electron and phonon operators, respectively, ε_i is the electronic energy, ω_λ is the phonon frequency, and $c_{i\lambda}$ is the electron–phonon coupling constant. Note that the frequency of the vibrational mode under consideration is assumed to remain unchanged after the electronic transition. The interaction Hamiltonian between the external field and the molecule, $\widehat{V}$, is represented using the rotating-wave approximation as

$$\widehat{V}(t) = \sum_{i>j} [\mu_{ij}^-(t) \hat{a}_i^\dagger \hat{a}_j^+ \mu_{ji}^+(t) \hat{a}_j^\dagger \hat{a}_i], \tag{A.3}$$

where

$$\mu_{ij}^-(t) = \mu_{ij}^- e_\alpha(t) \exp(-\mathrm{i}\Omega_\alpha t), \tag{A.4}$$

$$\mu_{ij}^- = \frac{1}{2} d_{ij} E_\alpha^*, \tag{A.5}$$

$$\mu_{ji}^+(t) = \mu_{ij}^-(t)^*, \tag{A.6}$$

and

$$e_\alpha(t) = \pi^{-1/4} \exp[-u_\alpha^2 (t - T_\alpha)^2/2]. \tag{A.7}$$

Here d_{ij} is the dipole moment of an electronic transition, and E_α ($\alpha = \mathrm{u}, \mathrm{r}$) denotes the field amplitudes for the pump (E_u) and probe (E_r) pulses. Ω_α and u_α^{-1} are the central frequency and pulse duration of those pulses, respectively. T_α is the time of the pulse arrival. Let us consider a simpler model, in which only a single vibrational mode is involved, and assume that its frequency remains unchanged after the electronic transition, namely the curvatures of the ground- and excited-state potential curves are identical. The pump pulse interacts with the system at $t = 0$. The probe pulse then arrives with a time delay T. By use of the fourth-order perturbation theory in terms of the field amplitude, the population in $|3\rangle$ is found to be

$$\begin{aligned} p_3 = {} & |\mu_{12}|^2 |\mu_{23}|^2 \pi^{-1} \hbar^{-4} N^{-1} \int_{-\infty}^{\infty} \mathrm{d}t_1 \int_{-\infty}^{t_1} \mathrm{d}t_2 \int_{-\infty}^{\infty} \mathrm{d}t_4 \int_{-\infty}^{t_4} \mathrm{d}t_3 \\ & \times \exp\left[-\frac{u_\mathrm{r}^2}{2}(t_1 - T)^2 - \frac{u_\mathrm{u}^2}{2} t_2^2 - \frac{u_\mathrm{u}^2}{2} t_3^2 - \frac{u_\mathrm{r}^2}{2}(t_4 - T)^2 \right. \\ & \left. + i\delta_\mathrm{r}(t_1 - t_4) + \mathrm{i}\delta_\mathrm{u}(t_2 - t_3) \right] \\ & \times \mathrm{Tr}(\widehat{D}_{32}(t_1) \widehat{D}_{21}(t_2) \rho_0 \widehat{D}_{21}^\dagger(t_3) \widehat{D}_{32}^\dagger(t_4)). \end{aligned} \tag{A.8}$$

Here ρ_0 is the initial vibrational density matrix, and N is the normalization factor. The detuning for the transitions induced by pump (u) and probe (r) pulses are given by

$$\delta_\alpha = \varepsilon_i/\hbar - \varepsilon_j/\hbar - \Omega_\alpha \tag{A.9}$$

with a set of parameters $(\alpha, i, j) = (\mathrm{u}, 2, 1)$, or $(\mathrm{r}, 3, 2)$. Here ε_i and Ω_α are the energy of the ith electronic state and the central frequency of the external electric field, respectively. The vibrational displacement operator, $\widehat{D}_{ij}$, can be expressed in terms of phonon operators, $\hat{b}^\dagger$ and $\hat{b}$, as

$$\widehat{D}_{ij} = \exp(g_{ij}(\hat{b}^\dagger - \hat{b})), \tag{A.10}$$

with the difference $g_{ij} = c_i - c_j$ in the electron–phonon coupling constants, c_i (i=1, 2, and 3). Pump and probe pulses are assumed to have an identical time duration, u_α^{-1}, and their electric field amplitudes are E_α. Dipolar interactions, $\mu_{ij} = \frac{1}{2} d_{ij} E_\alpha$, are given by the transition dipole moment d_{ij}.

References

[1] E. Schreiber, Femtosecond Real-time Spectroscopy of Small Molecules and Clusters, Springer, Berlin, 1998.
[2] A.H. Zewail, Ultrafast chemical and physical processes in molecular systems, in: M. Chergui (Ed.), Femtochemistry, World Scientific, Singapore, 1996, p. 3.
[3] A.H. Zewail, Ultrafast dynamics of the chemical bond, Femtochemistry, World Scientific, Singapore, 1994.
[4] C.J. Bardeen, Q. Wang, C.V. Shank, J. Phys. Chem. A 102 (1998) 2759.
[5] T. Kobayashi, A. Shirakawa, T. Fuji, IEEE J. Sel. Top. Quantum Electron. 7 (2001) 525.
[6] T. Fuji, H.J. Ong, T. Kobayashi, Chem. Phys. Lett. 380 (2003) 135.
[7] T. Kobayashi, A. Shirakawa, H. Matsuzawa, H. Nakanishi, Chem. Phys. Lett. 321 (2000) 525.
[8] S. Nakashima, Y. Nagasawa, K. Seike, T. Okada, M. Sato, T. Kohzuma, Chem. Phys. Lett. 331 (2000) 396.
[9] T. Kobayashi, T. Saito, H. Ohtani, Nature 414 (2001) 531.
[10] I. Martini, G.V. Hartland, Chem. Phys. Lett. 258 (1996) 180.
[11] C. Woywod, W.C. Livinghood, J.C. Frederick, J. Chem. Phys. 112 (2000) 626.
[12] V. Kimberg, F.F. Guimaraes, V.C. Felicissimo, F. Gel'mukhanov, Phys. Rev. A 73 (2006) 023409.
[13] T.S. Rose, M.J. Rosker, A.H. Zewail, J. Chem. Phys. 91 (1989) 7415.
[14] M. Yoshizawa, Y. Hattori, T. Kobayashi, Phys. Rev. B 47 (1993) 3882.
[15] M. Yoshizawa, Y. Hattori, T. Kobayashi, Phys. Rev. B 47 (1994) 13259.
[16] M. Yoshizawa, K. Nishiyama, M. Fujihira, T. Kobayashi, Chem. Phys. Lett. 207 (1993) 461.
[17] A. Kuehl, W. Domcke, J. Chem. Phys. 116 (2002) 263.
[18] D. Egorova, W. Domcke, Chem. Phys. Lett. 384 (2004) 1.
[19] T. Taneichi, T. Kobayashi, Y. Otsuki, Y. Fujimura, Chem. Phys. Lett. 231 (1994) 50.
[20] H. Koeppel, W. Domcke, L.S. Cederbaum, Adv. Chem. Phys. 57 (1984) 59.
[21] R. Schneider, W. Domcke, H. Koeppel, J. Chem. Phys. 92 (1990) 1045.
[22] H. Koeppel, L.S. Cederbaum, W. Domcke, J. Chem. Phys. 89 (1988) 2023.
[23] Z. Wang, T. Ohtsubo, T. Kobayashi, Chem. Phys. Lett. 430 (2006) 45.
[24] H. Kano, T. Kobayashi, J. Chem. Phys. 116 (2002) 184.
[25] C.V. Shank, R. Yen, R.L. Fork, J. Orenstein, G.L. Baker, Phys. Rev. Lett. 49 (1982) 1660.
[26] C.V. Shank, R. Yen, J. Orenstein, G.L. Baker, Phys. Rev. B 28 (1983) 6095.
[27] L. Rothberg, T.M. Jedju, S. Etemad, G.L. Baker, IEEE J. Quantum Electron. 24 (1988) 311.
[28] L. Rothberg, T.M. Jedju, P.D. Townsend, S. Etemad, G.L. Baker, Mol. Cryst. Liq. Cryst. 194 (1991) 1.
[29] Z.V. Vardeny, Chem. Phys. 177 (1993) 743.
[30] R. Kohlrausch, Ann. Phys. 12 (1847) 392.
[31] A.T.N. Kumar, F. Rosca, A. Widom, P.M. Champion, J. Chem. Phys. 114 (2001) 701.
[32] P.W. Atkins, Quanta: A Handbook of Concepts, 2nd ed., Oxford University Press, UK, 1991.
[33] J. Janszky, P. Adam, A.V. Vinogradov, T. Kobayashi, Spectrochim. Acta 48 A (1992) 31.
[34] T. Taneichi, J. Janszky, T. Kobayashi, Chem. Phys. Lett. 419 (2006) 540.
[35] Z. Lan, W. Domcke, V. Vallet, A.L. Sobolewski, S. Mahapatra, J. Chem. Phys. 122 (2005) 224315.
[36] M. Abe, Y. Ohtsuki, Y. Fujimura, W. Domcke, J. Chem. Phys. 123 (2005) 144508.
[37] M. Abe, Y. Ohtsuki, Y. Fujimura, Z. Lan, W. Domcke, J. Chem. Phys. 124 (2006) 224316.
[38] Z. Sun, N. Lou, G. Nyman, Chem. Phys. 308 (2005) 317.
[39] T. Taneichi, T. Fuji, Y. Yuasa, T. Kobayashi, Chem. Phys. Lett. 394 (2004) 377.
[40] F. Araoka, unpublished result.
[41] J. Janszky, T. Kobayashi, An.V. Vinogradov, Opt. Commun. 76 (1990) 30.
[42] J. Janszky, Y.Y. Yushin, Opt. Commun. 59 (1986) 151.
[43] J. Janszky, An.V. Vinogradov, Phys. Rev. Lett. 64 (1989) 2771.
[44] M.D. Feit, J.A. Fleck, A. Steiger, J. Comput. Phys. 47 (1982) 412.